

ARTICLE

DOI: 10.1038/s41467-018-03341-6

OPEN

# Ruthenium(II)-enabled *para*-selective C–H difluoromethylation of anilides and their derivatives

Chunchen Yuan<sup>1</sup>, Lei Zhu<sup>2</sup>, Changpeng Chen<sup>1</sup>, Xiaolan Chen<sup>1</sup>, Yong Yang<sup>3</sup>, Yu Lan<sup>2</sup> & Yingsheng Zhao<sup>1</sup>

Transition-metal-catalyzed direct site-selective functionalization of arene C–H bonds has emerged as an innovative approach for building the core structure of pharmaceutical agents and other versatile complex compounds. However, *para*-selective C–H functionalization has seldom been explored, only a few examples, such as steric-hindered arenes, electron-rich arenes, and substrates with a directing group, have been reported to date. Here we describe the development of a ruthenium-enabled *para*-selective C–H difluoromethylation of anilides, indolines, and tetrahydroquinolines. This reaction tolerates various substituted arenes, affording *para*-difluoromethylation products in moderate to good yields. Results of a preliminary study of the mechanism indicate that chelation-assisted cycloruthenation might play a role in the selective activation of *para*-C<sub>Ar</sub>-H bonds. Furthermore, this method provides a direct approach for the synthesis of fluorinated drug derivatives, which has important application for drug discovery and development.

<sup>1</sup>Key Laboratory of Organic Synthesis of Jiangsu Province College of Chemistry, Chemical Engineering, and Materials Science Soochow University, Suzhou 215123, China. <sup>2</sup>School of Chemistry and Chemical Engineering Chongqing University, Chongqing 40030, China. <sup>3</sup>Qingdao Institute of Bioenergy and Bioprocess Technology, Chinese Academy of Science, Qingdao 266000, China. Correspondence and requests for materials should be addressed to Y.L. (email: lanyu@cqu.edu.cn) or to Y.Z. (email: yszhao@suda.edu.cn)

Over the past decade, transition-metal-catalyzed direct site-selective functionalization of arene C–H bonds has emerged as an innovative approach for building the core structure of pharmaceutical agents and other versatile complex compounds. In this context, various *ortho*-selective C–H functionalization reactions have been well-developed through the  $\sigma$ -chelation-directed cyclometalation strategy<sup>1–9</sup>. However, remote C–H functionalization still remains a great challenge. Compared with recently developed *meta*-selective C–H functionalization<sup>10–26</sup>, *para*-selective C–H functionalization is less explored;<sup>27–34</sup> only a few examples, such as steric-hindered arenes<sup>35,36</sup>, electron-rich arenes<sup>37–43</sup>, and substrates with a directing group<sup>44</sup>, have been reported to date. For instance, Zhang and co-workers reported in 2011 a Pd(II)-catalyzed *para*-selective amination of *ortho*-methoxy-substituted anilide. Interestingly, substrate blockage of both *ortho*-positions was also tolerated (Fig. 1a). In 2015, Maiti's group independently developed a D-shaped template for the highly selective olefination of the *para*-C–H bond using a palladium catalyst (Fig. 1a)<sup>45</sup>. Very recently, a variety of *para*-selective functionalizations of less-activated arenes via nickel/aluminum<sup>46</sup>, gold<sup>47</sup>, and palladium<sup>48</sup> catalyzes have been reported. Despite such major advances, most *para*-selective C–H functionalizations suffer from serious drawbacks such as limited substrate scope and relatively poor regioselectivity, which significantly restrict their applications (Fig. 1a)<sup>27–34</sup>. Therefore, a catalyst-controlled strategy for *para*-selective C–H functionalization of arenes is highly desired.

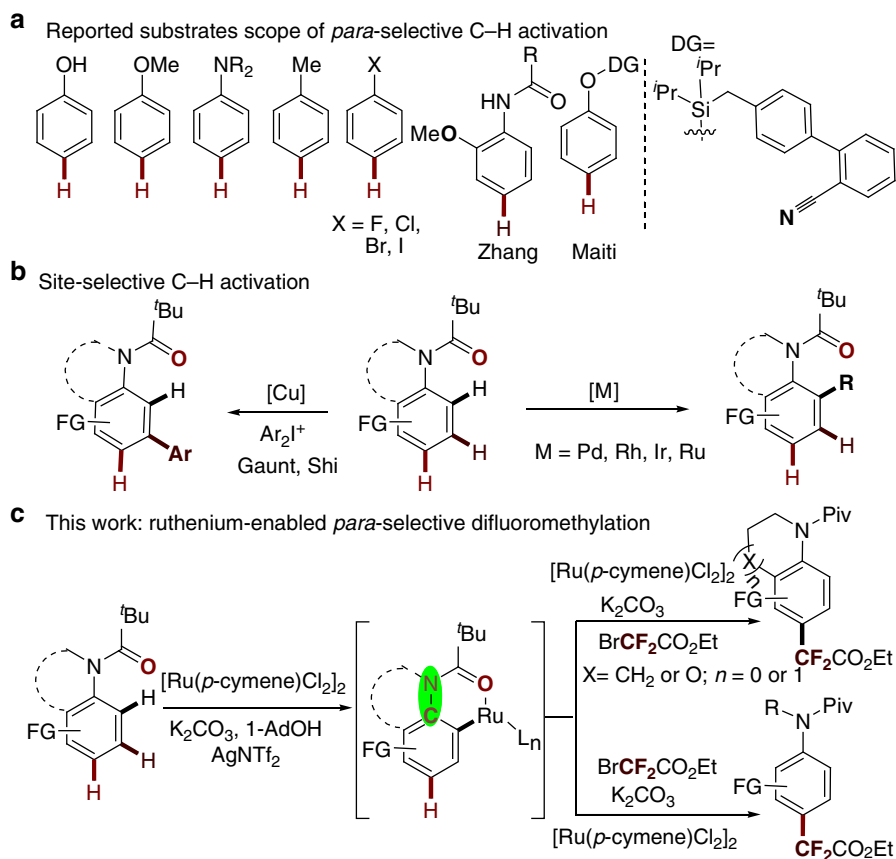
Fluorine-containing compounds are widely applied in pharmaceuticals, agrochemicals, and life sciences<sup>49,50</sup>. Specifically, the installation of a difluoromethylene (CF<sub>2</sub>) group into organic compounds is of particular value because it can cause significant

changes in the chemical and physical properties of biologically active compounds<sup>51,52</sup>. As a consequence, there is a continued strong demand for methods that enable the selective synthesis of difluoromethylated molecules<sup>53–56</sup>.

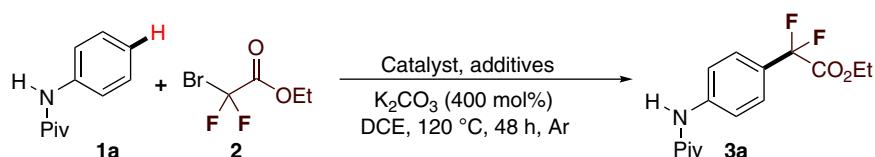
Despite the development of various approaches to *ortho*- and *meta*-selective C–H functionalizations of anilides, indolines, and tetrahydroquinolines, which are significantly important molecular skeletons in medicinal chemistry (Fig. 1b)<sup>57–62</sup>, the general strategy for highly *para*-selective C–H functionalization is still elusive. Herein, we report a ruthenium(II)-enabled *para*-selective difluoromethylation of anilides, indolines, and tetrahydroquinolines. This reaction tolerates a wide variety of functional groups, affording the corresponding *para*-difluoromethylated products in moderate to good yields. Preliminary experimental results suggest that chelation-assisted cycloruthenation might play a role in the selective activation of *para*-C<sub>Ar</sub>–H bonds.

## Results

**Optimization of reaction conditions.** At the outset, *N*-pivaloylaniline **1a** was reacted with bromodifluoroacetate **2** in the presence of [Ru(*p*-cymene)Cl<sub>2</sub>]<sub>2</sub> (5 mol%), 1-Ad-OH (0.2 equiv.), and K<sub>2</sub>CO<sub>3</sub> (4 equiv.) in DCE at 120 °C to investigate whether the *para*-selective C–H difluoromethylation could be performed. We were pleased to observe that we generated the *para*-difluoromethylated product **3a** in 45% yield (Table 1, entry 1). Encouraged by this result, we decided to further optimize the conditions to improve the efficiency. We investigated several additives, e.g., MesCO<sub>2</sub>H, Piv-Val-OH, Piv-OH, and KOAc, but none of them gave a noticeable enhancement (Table 1, entries



**Fig. 1** Site-selective C–H activation reactions. **a** Reported substrate scope of *para*-selective C–H activation. **b** Site-selective C–H activation. **c** Our work on ruthenium-enabled *para*-selective difluoromethylation

**Table 1 Optimization of *para*-C-H difluoromethylation<sup>a</sup>**

Entry	Catalyst (5 mol%)	Silver salt (10 mol%)	Additive (20 mol%)	Yield (%) <sup>b</sup>
1	[Ru( <i>p</i> -cymene)Cl <sub>2</sub> ] <sub>2</sub>	No	1-Ad-OH	45
2	[Ru( <i>p</i> -cymene)Cl <sub>2</sub> ] <sub>2</sub>	No	KOAc	35
3	[Ru( <i>p</i> -cymene)Cl <sub>2</sub> ] <sub>2</sub>	No	Piv-OH	39
4	[Ru( <i>p</i> -cymene)Cl <sub>2</sub> ] <sub>2</sub>	No	MesCO <sub>2</sub> H	40
5	[Ru( <i>p</i> -cymene)Cl <sub>2</sub> ] <sub>2</sub>	No	Piv-Val-OH	32
6	[Ru( <i>p</i> -cymene)Cl <sub>2</sub> ] <sub>2</sub>	AgBF <sub>4</sub>	1-Ad-OH	51
7	[Ru( <i>p</i> -cymene)Cl <sub>2</sub> ] <sub>2</sub>	AgSbF <sub>6</sub>	1-Ad-OH	48
8	[Ru( <i>p</i> -cymene)Cl <sub>2</sub> ] <sub>2</sub>	AgNTf <sub>2</sub>	1-Ad-OH	65
9	[Ru( <i>p</i> -cymene)Cl <sub>2</sub> ] <sub>2</sub>	AgNTf <sub>2</sub>	1-Ad-OH	87 <sup>c</sup>
10	RuCl <sub>3</sub>	AgNTf <sub>2</sub>	1-Ad-OH	21 <sup>c</sup>
11	Pd(PPh <sub>3</sub> ) <sub>4</sub>	No	1-Ad-OH	Trace
12	Cu <sub>2</sub> O	No	1-Ad-OH	Trace
13	Ni(acac) <sub>2</sub>	No	1-Ad-OH	Trace
14	No	AgNTf <sub>2</sub>	1-Ad-OH	0

<sup>a</sup> Reaction condition: 1a (0.20 mmol, 1.0 equiv.), 2 (3 equiv.), K<sub>2</sub>CO<sub>3</sub> (4 equiv.), catalyst (5 mol%), additive (20 mol%), and Ag salt (10 mol%) in DCE (0.5 mL) for 48 h at 120 °C under argon in a sealed tube

<sup>b</sup> GC yield using biphenyl as the internal standard

<sup>c</sup> Ag salt (20 mol%)

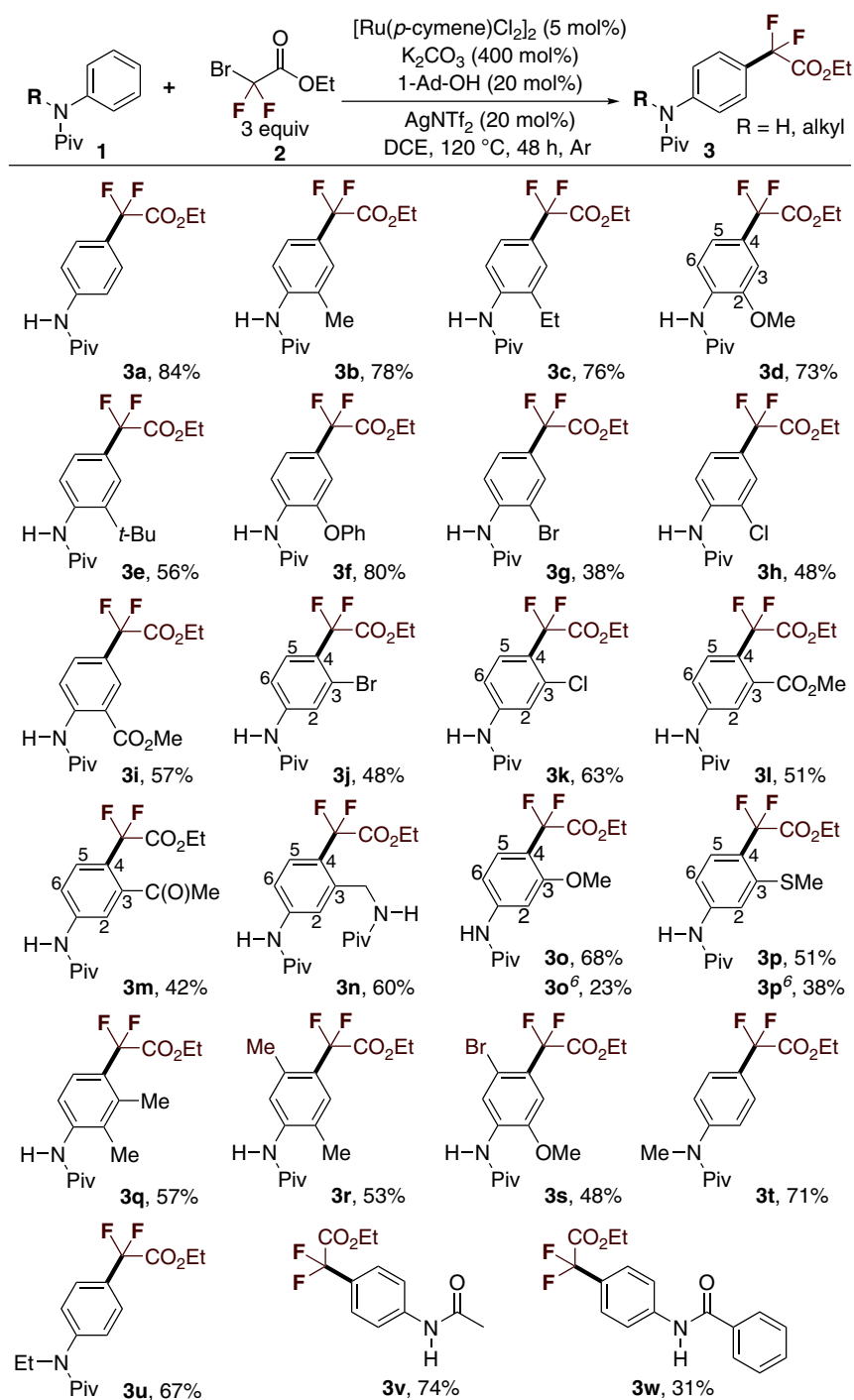
2–5). Subsequently, various silver salts that are known as facilitating to activate the rhodium or iridium catalyst precursors were screened. To our great delight, dramatically improved yields of **3a** were obtained (53–65%; Table 1, entries 6–8). We could further enhance the reaction efficiency by an increase in AgNTf<sub>2</sub> (20 mol %) loading, which provided product **3a** in 87% yield (Table 1, entry 9). In addition, the use of RuCl<sub>3</sub>, Pd(PPh<sub>3</sub>)<sub>4</sub>, or Cu<sub>2</sub>O, Ni(acac)<sub>2</sub> or the obviation of [Ru(*p*-cymene)Cl<sub>2</sub>]<sub>2</sub> failed to lead to *para*-selective transformation under otherwise identical conditions (Table 1, entries 10–14).

**Scope of the anilide derivatives.** Having identified the optimal reaction conditions, we next investigated the substrate scope to explore the versatility of this *para*-selective difluoromethylation protocol (Table 2). First, a series of *ortho*-substituted *N*-phenylpivalamides (**1a–1i**) performed well under the standard conditions; the corresponding *para*-difluoromethylated products **3a–3i** were exclusively obtained in yields of 38–84% along with the recovered starting material. Various functional groups, such as Me, Et, OMe, OPh, *t*-Bu, Cl, Br, and CO<sub>2</sub>Me, were fully tolerated. A sterically hindered functional group (*t*Bu, **1e**) and electron-withdrawing substituents (Cl, Br, CO<sub>2</sub>Me, **1g–1i**) gave slightly inferior yields. It is noteworthy that *o*-methoxy-substituted *N*-phenylpivalamides (**1d**) were exclusively transformed into *p*-difluoromethylated products (**3d**) without formation of the product difluoromethylated at the C5 position. Subsequently, *meta*-substituted *N*-phenylpivalamides (**1j–1p**) were used in the reaction. Overall, the reaction tolerated a wide range of functional groups at the *meta* position and afforded a decent yield with excellent regioselectivity. The difluoromethylation was found to prefer sterically bulkier positions (C4) over the less sterically hindered positions (C5). Of note are the exceptions, the *meta*-substituted substrates **1o** and **1p**, which afforded a mixture of *ortho*- and *para*-difluoromethylated products, respectively. It is

probable that the electron-donating effect of the methoxy or methylthio groups greatly influenced the reactivity of the C–Ru bonds. Thus, the ruthenium(II) complex could successively trap electrophilic ·CF<sub>2</sub>CO<sub>2</sub>Et radicals and undergo reductive elimination, affording *ortho*-difluoromethylated products (**3o**<sup>(6)</sup>, **3p**<sup>(6)</sup>). Moreover, the steric effect of the thiomethyl group resulted in a low yield of *para*-difluoromethylated product **3p**. Moreover, all of the disubstituted substrates **3q–3s** performed well, providing the *para*-difluoromethylated products in good yields.

These results might indicate that site selectivity is controlled by ruthenium catalysis rather than by functional groups on the aromatic ring. This *para*-selective difluoromethylation protocol is also amenable to *N*-alkylanilines protected with pivaloyl amide. All of the substrates reacted well under standard conditions, affording the *para*-difluoromethylated products in satisfactory yields (**3t**, **3u**). However, *ortho*- and *meta*-trifluoromethyl-substituted phenylpivalamides were less reactive, affording difluoromethylated products in only trace amounts (Supplementary Figs. 3–7). When acetyl- and benzoyl-protected aniline were subjected to standard reaction conditions, the difluoromethylated products were obtained in moderate to good yields (**3v**, **3w**). We were puzzled as to how the substrates with a small, strongly electronegative fluorine substituted pivaloyl amide either at the *ortho* or *meta* position, providing exclusively *ortho*-difluoromethylated products (Supplementary Figs. 2, **3sa**, **3sb**) in good yields. We may attribute this to the electron-withdrawing effect of fluorine, which suppressed the directing ability of *ortho* cycloruthenation and thereby caused selectivity toward different sites (Supplementary Figs. 3–10).

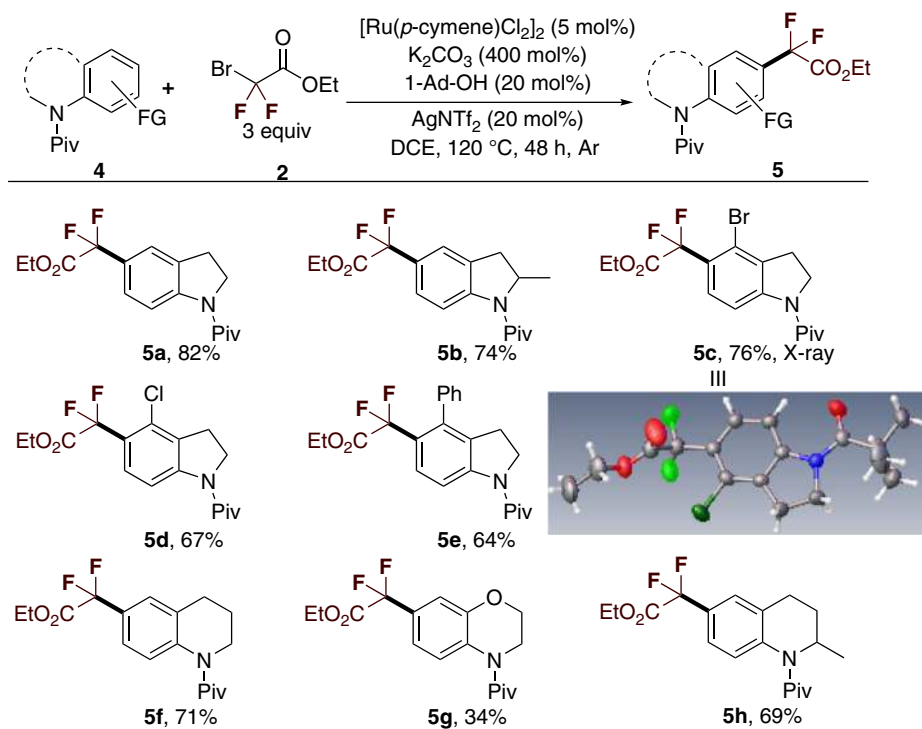
**Scope of the substrates indolines and tetrahydroquinolines.** The structural units indoline and tetrahydroquinolines are highly important molecular skeletons in medicinal chemistry; they are widely found in several well-known drugs, such as indapamide,

**Table 2 Substrate scope of anilides<sup>a</sup>**

<sup>a</sup> Reaction conditions: [Ru(*p*-cymene)Cl<sub>2</sub>]<sub>2</sub> (5 mol%), **1** (0.20 mmol, 1.0 equiv.), K<sub>2</sub>CO<sub>3</sub> (4 equiv.), 1-Ad-OH (20 mol%), AgNTf<sub>2</sub> (20 mol%), and **2** (3 equiv.) in DCE (0.5 mL) at 120 °C for 48 h under argon; isolated yield after chromatography

ajmaline, oxamniquine, and argatroban. To explore the generality of this protocol, a number of indoline and tetrahydroquinoline derivatives protected with pivaloyl amide were used as substrates for *para*-selective difluoromethylation. Gratifyingly, all of these substrates were also compatible with the reaction, delivering the desired *para*-difluoromethylated products in moderate to good yields (Table 3). A set of functional groups, such Me, Cl, Br, and Ph, were all tolerated by this procedure. It is worth mentioning

that the single-crystal structure of product **5c** confirms that the ruthenium-enabled difluoromethylation selectively occurs at the *para* position. In addition, we extended the reaction to mono-fluoromethylation and non-fluoromethylation, but we obtained only <20% yields of the corresponding products under harsh reaction conditions (Fig. 2). This result may be attributed to the stability of the corresponding free radicals.

**Table 3 Substrate scope of indolines and tetrahydroquinolines<sup>a</sup>**

<sup>a</sup> Reaction conditions: [Ru(*p*-cymene)Cl<sub>2</sub>]<sub>2</sub> (5 mol%), **1** (0.20 mmol, 1.0 equiv.), K<sub>2</sub>CO<sub>3</sub> (4 equiv.), 1-Ad-OH (20 mol%), AgNTf<sub>2</sub> (20 mol%), and **2** (3 equiv.) in DCE (0.5 mL) at 120 °C for 48 h under argon; isolated yield after chromatography

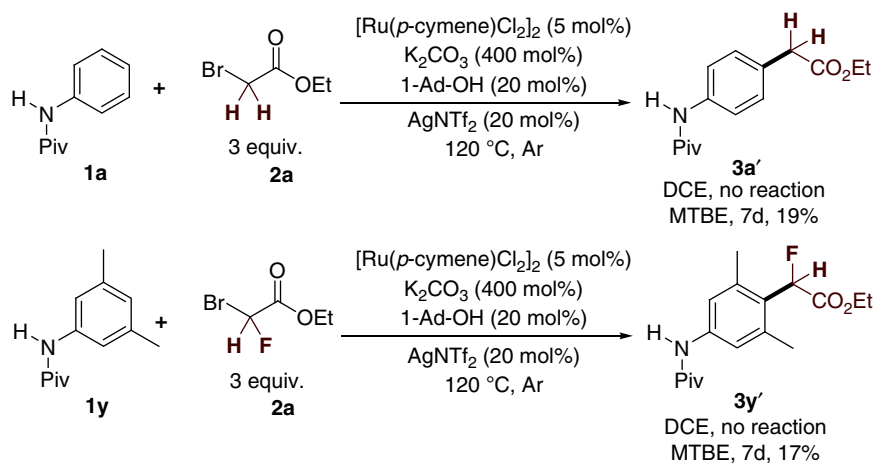


**Fig. 2** Mono- and non-fluoromethylation. **a** Ruthenium(II)-enabled *para*-selective non-fluoromethylation. **b** Ruthenium(II)-enabled *para*-selective mono-fluoromethylation

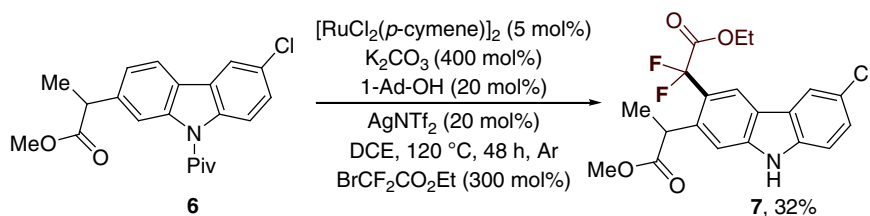


**Fig. 3** The application in organic synthesis. Synthesis of a carprofen derivative

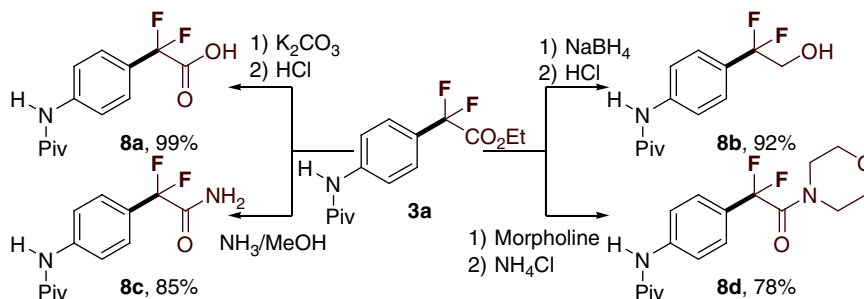


**Fig. 4** Transformations of **3a**. All the reactions were performed in 0.2 mmol scale. Isolated yields. **a**  $\text{K}_2\text{CO}_3$ , MeOH, 60 °C. **b**  $\text{NaBH}_4$ , EtOH, r.t. **c**  $\text{NH}_3$ , MeOH, 60 °C. **d** Morpholine, 60 °C

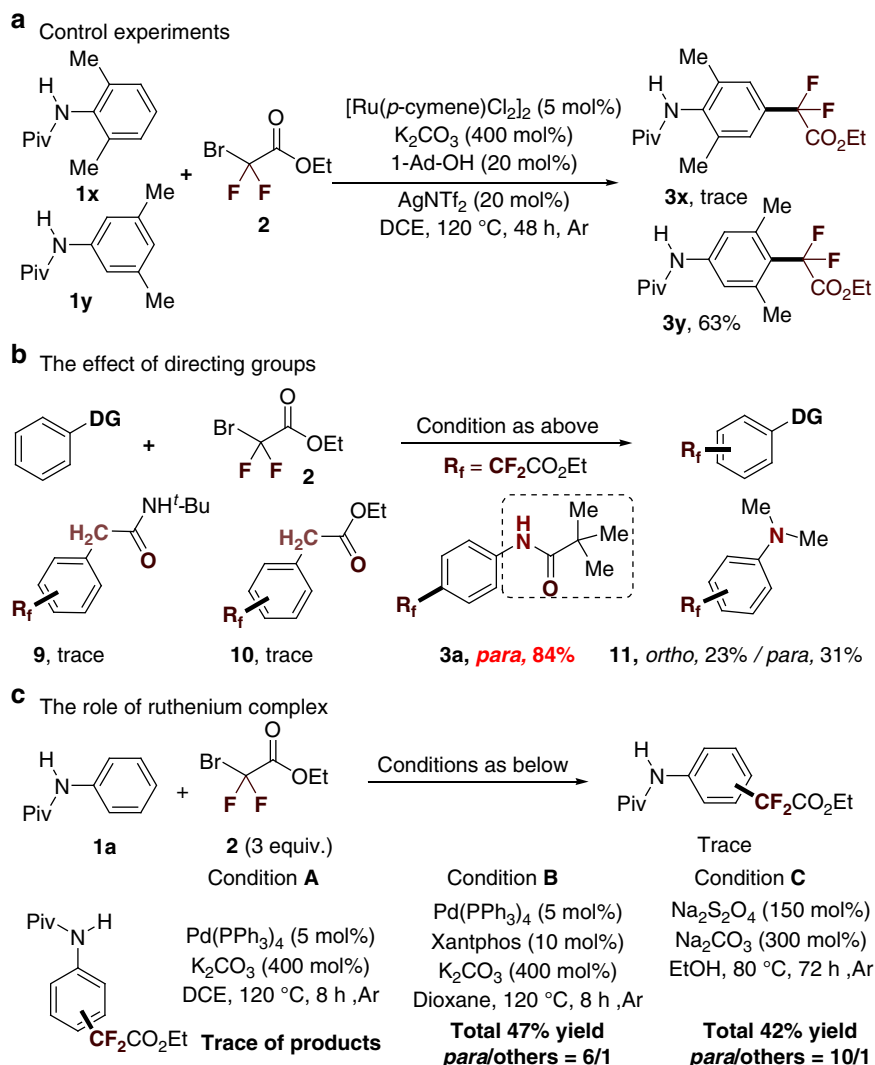


**Fig. 5** Preliminary studies on the mechanism. **a** Control experiments. **b** The effect of directing group. **c** The role of ruthenium complex

The importance and utility of this protocol can be highlighted by the synthesis of leflunomide (Supplementary Fig. 13), and a carprofen derivative (Fig. 3)<sup>63,64</sup>, which is a non-steroidal anti-inflammatory drug. Because of the possible decomposition of carprofen protected with pivaloyl amide in the reaction, a relatively low yield of **7** was afforded. Furthermore, the aryl difluoroacetates could be used as precursors to access a variety of difluoromethyl-containing organic molecules such as carboxylic acid (Fig. 4, **8a**), primary alcohol (Fig. 4, **8b**), and amides (Fig.

4, **8c–8d**) in high yields, through different known procedures, as illustrated in Fig. 3. As demonstrated earlier, this method may be a unique and highly efficient protocol for drug discovery and development (Fig. 4).

**Mechanistic investigations.** To understand the reaction pathway of this ruthenium-catalyzed site-selective difluoromethylation reaction, additional experiments were extensively performed.

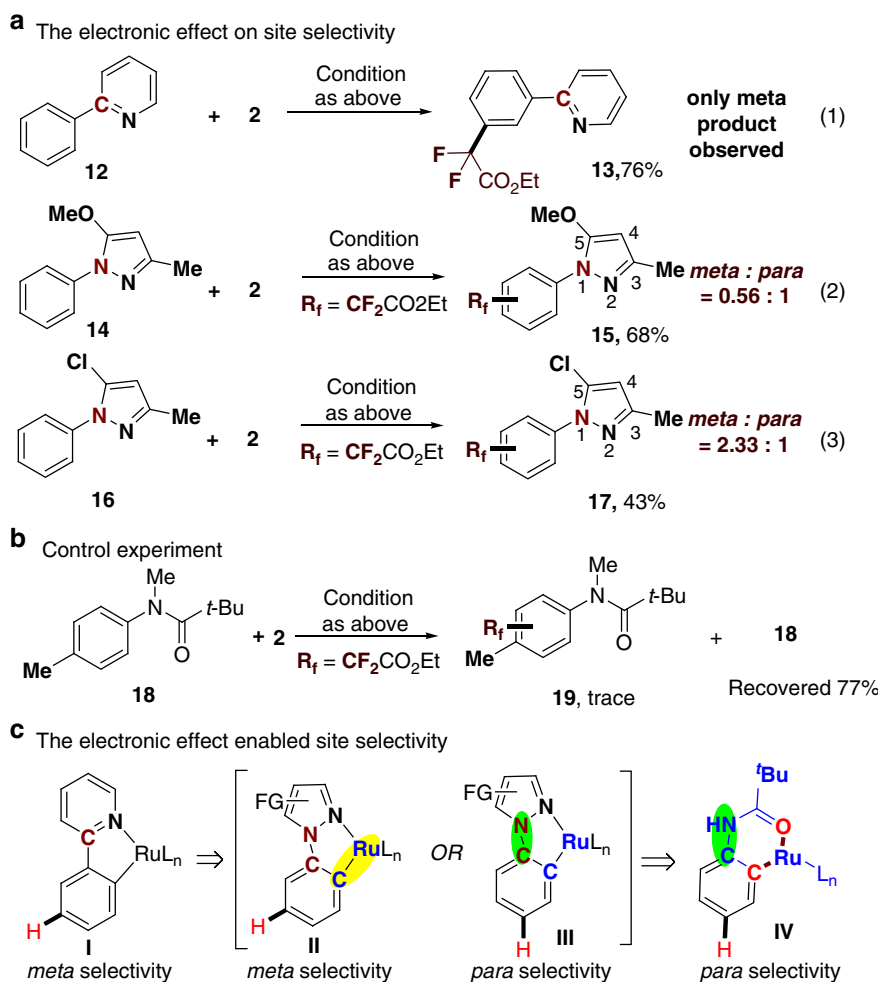


**Fig. 6** Preliminary studies on site selectivity. **a** The electronic effect on site selectivity. **b** Control experiment. **c** The electronic enabled site selectivity

First, a control experiment was conducted by using 2,6-dimethyl-substituted aniline as a substrate under the standard conditions (Fig. 5, **1x**). In this case, no desired product was formed and the starting material was completely recovered. In sharp contrast, the pivaloyl amide protected 3,5-dimethylaniline (Fig. 5, **1y**) gave the *para*-difluoromethylated products **3y** in 63% yield (Fig. 5a). Second, no formation of difluoromethylated products were obtained when ethylphenyl acetate and *N*-(*tert*-butyl)-2-phenylacetamide were coupled with **2** under standard conditions (Fig. 5b). Interestingly, the reaction of *N,N*-dimethylaniline<sup>37</sup> as a substrate proceeded well but afforded a mixture of *ortho*- and *para*-difluoromethylated products **11** (*ortho/para* ratio = 1:1.4). These results indicate that *ortho*-C<sub>Ar</sub>-H metalation plays an important role in accessing *para*-C-H functionalization reactions<sup>17</sup>. To further test this hypothesis, several other control experiments were performed (Fig. 5c). The  $\cdot\text{CF}_2\text{CO}_2\text{Et}$  radical can be generated from 2-bromo-2,2-difluoroacetates, as reported by the groups of Ackermann<sup>25</sup>, Wang<sup>26</sup>, and Kondratov<sup>65</sup>. Thus, we directly treated the substrate **1a** with **2** in the presence of the radical initiator. Interestingly, we found that the difluoromethyl radical could be trapped by the substrate **1a**. However, only a mixture of *ortho*-, *meta*-, and *para*-difluoromethylated products were obtained. These results suggest that the arylruthenium intermediate (Fig. 6c, IV) might play a role in realizing the *para* selectivity.

Third, a set of parallel experiments were performed in order to gain insights into the *para* selectivity (Fig. 6). We found that only

the *meta*-difluoromethylated product **13** was generated in 76% yield when 2-phenylpyridine (**12**) and bromodifluoroacetate (**2**) were treated under standard conditions (Fig. 6a, Eq. (1)). This result is consistent with the reports of Ackermann and Wang on *meta*-selective difluoromethylation<sup>25,26</sup>. However, when the pyrazole derivative **14** was utilized in the reaction, a mixture of *meta*- and *para*-difluoromethylated products **15** (0.56:1) was obtained in 68% total yield (Fig. 6, Eq. (2)). Interestingly, a decrease in the electron-donating effect on N<sub>1</sub> in the pyrazole ring significantly resulted in the regioselectivity shift from the *para*- to the *meta*-position (Fig. 6, Eqs. (2) and (3)). These results clearly indicate that the site selectivity could be elegantly tuned by modifying the electronic effect of N<sub>1</sub>. Finally, pivaloyl amide protected *N*-methyl-*p*-toluidine **18**, in which the *para* position was blocked with a -Me group, only afforded <5% yield of difluoromethylated products, along with 77% recovery of the starting material (Fig. 6b), indicating that the ruthenium-catalyzed C-H functionalizations tend to occur at the *para*-C<sub>Ar</sub>-H position of anilides.

The *para* difluoromethylation of the isotopically labeled substrate was investigated (Fig. 7). We found that treating **1a**-[D<sub>5</sub>] with **2** under standard reaction conditions afforded the product **3a**-[D] in 83% yield, with significant D/H scrambling at the *ortho* position. A similar D/H scrambling result was observed when **1a**-[D<sub>5</sub>] was subjected to standard reaction conditions without **2** (Fig. 7a). This result indicates that *orthocycloruthenation* is reversible. The observed kinetic isotope effect value of 1.0

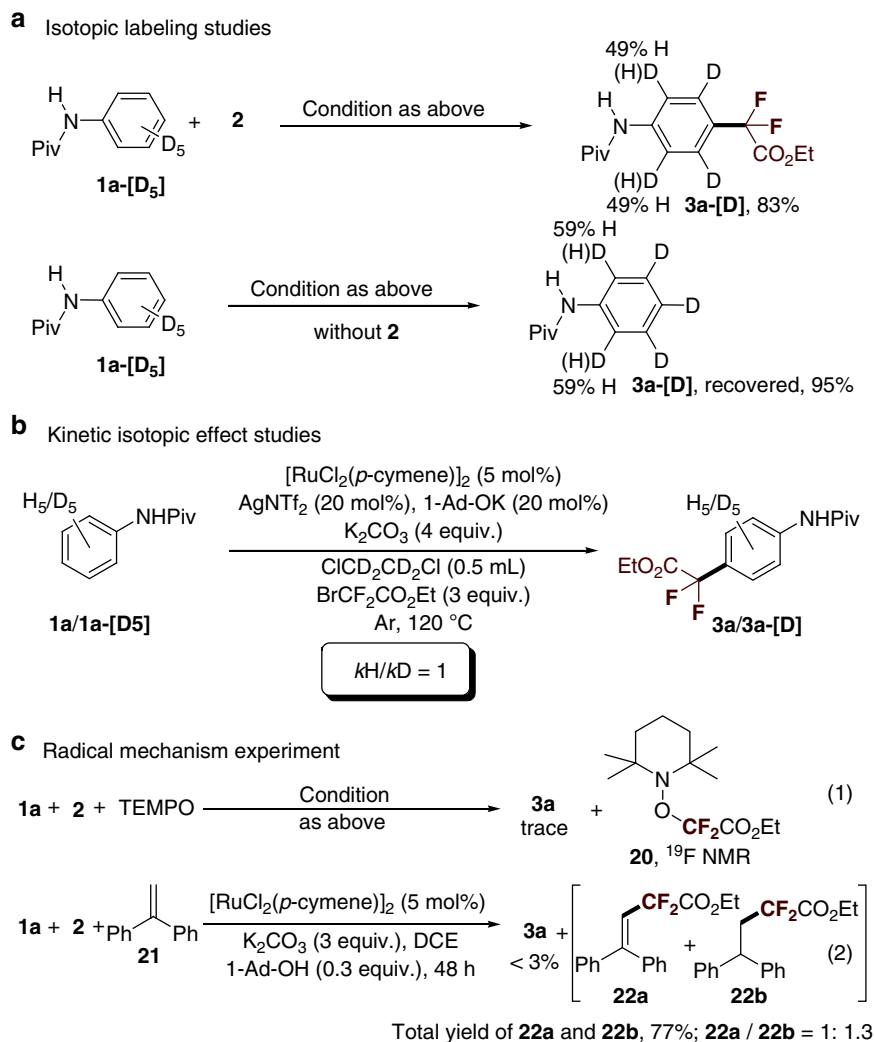


**Fig. 7** Deuteration and radical experiments. **a** Isotopic labeling studies. **b** Kinetic isotopic effect studies. **c** Radical mechanism experiment

(Fig. 7b) suggests that  $C_{Ar}$ -H activation is not a kinetically relevant step. Next, we tried to explore the nature of the *para*-carbon-carbon bond formation using **2**. The reaction conducted in the presence of the radical scavenger TEMPO resulted in complete inhibition of catalytic activity without formation of the desired product **3a**. A further  $^{19}\text{F}$  NMR study revealed that **20** may have been generated in the reaction, in good agreement with the results of Ackermann et al.<sup>25,26</sup>. We subsequently introduced the radical scavenger, 1,1-diphenylethylene (**21**)<sup>66,67</sup>, which could trap the  $\cdot\text{CF}_2\text{CO}_2\text{Et}$  radical generated in situ in the reaction (Fig. 7c). As expected, the products **22** formed by coupling **21** with  $\cdot\text{CF}_2\text{CO}_2\text{Et}$  were predominantly obtained in 77% total yield, and only a trace amount of **3a** was observed along with recovery of **1a** (Fig. 7c). We further treated **21** with **2** directly in the presence of ruthenium catalysts and  $\text{K}_2\text{CO}_3$  in 1,4-dioxane for 12 h in order to obtain a mixture of **22a** and **22b** in yields >40%. Taken together, all of the foregoing observations suggest the involvement of a free radical pathway for this *para*-selective difluoromethylation, in which the ruthenium(II) complex can release a  $\cdot\text{CF}_2\text{CO}_2\text{Et}$  radical through single-electron transfer with **2** as the oxidant.

## Discussion

In conclusion, we demonstrated the *para*-selective C-H difluoromethylations of various anilides and indolines using a

ruthenium catalyst. In addition, this method provides an efficient approach to directly access fluorinated bioactive compounds derivatives, which is significant for the development of new drugs. Preliminary experimental results show that the catalyst provides *para* selectivity and that it can release the electrophilic  $\cdot\text{CF}_2\text{CO}_2\text{Et}$  radical from ethylbromodifluoroacetate. Further applications and mechanistic studies including DFT calculations are now underway.

## Methods

**Procedure for Ru-catalyzed *para*-C-H difluoromethylation.** A mixture of **1** or **4** (0.2 mmol, 1.0 equiv.),  $\text{BrCF}_2\text{CO}_2\text{Et}$  (80  $\mu\text{L}$ , 121.2 mg, 3 equiv.),  $[\text{Ru}(p\text{-cymene})\text{Cl}_2]_2$  (6 mg, 5 mol%),  $\text{K}_2\text{CO}_3$  (108.8 mg, 400 mol %), 1-Ad-OH (7.2 mg, 20 mol%),  $\text{AgNTf}_2$  (14.4 mg, 20 mol%), and DCE (0.5 mL) in a 15 mL glass vial sealed under argon atmosphere was heated at 120 °C for 48 h. The reaction mixture was cooled to room temperature and concentrated in vacuo. The resulting residue was purified by column chromatography (PE/EA = 10: 1) on silica gel to give the product **3** or **5**. Full experimental details and characterization of new compounds can be found in the Supplementary Methods.

**Data availability.** The authors declare that all relevant data supporting the findings of this study are available within the article and its Supplementary Information files. The X-ray crystallographic coordinates for structures reported in this study have been deposited at the Cambridge Crystallographic Data Centre (CCDC), under deposition numbers 1513022. These data can be obtained free of charge from The Cambridge Crystallographic Data Centre via [www.ccdc.cam.ac.uk/data\\_request/cif](http://www.ccdc.cam.ac.uk/data_request/cif).



Received: 17 May 2017 Accepted: 25 January 2018

Published online: 22 March 2018

## References

- Giri, R., Shi, B.-F., Engle, K. M., Maugel, N. & Yu, J.-Q. Transition metal-catalyzed C–H activation reactions: diastereoselectivity and enantioselectivity. *Chem. Soc. Rev.* **38**, 3242–3272 (2009).
- Lyons, T. W. & Sanford, M. S. Palladium-catalyzed ligand-directed C–H functionalization reactions. *Chem. Rev.* **110**, 1147–1169 (2010).
- Wencel-Delord, J. & Glorius, F. C–H bond activation enables the rapid construction and late-stage diversification of functional molecules. *Nat. Chem.* **5**, 369–375 (2012).
- Ackermann, L. Carboxylate-assisted ruthenium-catalyzed alkyne annulations by C–H/Het–H bond functionalizations. *Acc. Chem. Res.* **47**, 281–295 (2014).
- He, G., Wang, B., Nack, W. A. & Chen, G. Syntheses and transformations of  $\alpha$ -amino acids via palladium-catalyzed auxiliary-directed  $sp^3$  C–H functionalization. *Acc. Chem. Res.* **49**, 635–645 (2016).
- Moselage, M., Li, J. & Ackermann, L. Cobalt-catalyzed C–H activation. *ACS Catal.* **6**, 498–525 (2016).
- Daugulis, O., Roane, J. & Tran, L. D. Bidentate, monoanionic auxiliary-directed functionalization of carbon–hydrogen bonds. *Acc. Chem. Res.* **48**, 1053–1064 (2015).
- Wencel-Delord, J. & Glorius, F. C–H bond activation enables the rapid construction and late-stage diversification of functional molecules. *Nat. Chem.* **5**, 369–375 (2013).
- Yeung, C. S. & Dong, V. M. Catalytic dehydrogenative cross-coupling: forming carbon–carbon bonds by oxidizing two carbon–hydrogen bonds. *Chem. Rev.* **111**, 1215–1292 (2011).
- Li, J. & Ackermann, L. C–H activation: following directions. *Nat. Chem.* **7**, 686–687 (2015).
- Juliá-Hernández, F., Simonetti, M. & Larrosa, I. Metalation dictates remote regioselectivity: ruthenium-catalyzed functionalization of meta  $C_{Ar}$ –H bonds. *Angew. Chem. Int. Ed.* **52**, 11458–11460 (2013).
- Leow, D., Li, G., Mei, T.-S. & Yu, J.-Q. Activation of remote meta-C–H bonds assisted by an end-on template. *Nature* **486**, 518–522 (2012).
- Tang, R.-Y., Li, G. & Yu, J.-Q. Conformation-induced remote meta-C–H activation of amines. *Nature* **507**, 215–220 (2014).
- Bera, M., Maji, A., Sahoo, S. K. & Maiti, D. Palladium(II)-catalyzed meta-C–H olefination: constructing multisubstituted arenes through homo-diolefinatation and sequential hetero-diolefinatation. *Angew. Chem. Int. Ed.* **54**, 8515–8519 (2015).
- Phipps, R. J. & Gaunt, M. J. A meta-selective copper-catalyzed C–H bond arylation. *Science* **323**, 1593–1597 (2009).
- Duong, H. A., Gilligan, E., Cooke, M. L., Phipps, R. J. & Gaunt, M. J. Copper(II)-catalyzed meta-selective direct arylation of  $\alpha$ -aryl carbonyl compounds. *Angew. Chem. Int. Ed.* **50**, 463–466 (2011).
- Fan, Z., Ni, J. & Zhang, A. Meta-selective  $C_{Ar}$ –H nitration of arenes through a  $Ru_3(CO)_{12}$ -catalyzed ortho-metalation strategy. *J. Am. Chem. Soc.* **138**, 8470–8475 (2016).
- Yu, Q., Hu, L. A., Wang, Y., Zheng, S. & Huang, J. Directed meta-selective bromination of arenes with ruthenium catalysts. *Angew. Chem. Int. Ed.* **54**, 15284–15288 (2015).
- Teskey, C. J., Lui, A. Y. W. & Greaney, M. F. Ruthenium-catalyzed meta-selective C–H bromination. *Angew. Chem. Int. Ed.* **54**, 11677–11680 (2015).
- Paterson, A. J., John-Campbell, S., Mahon, M. F., Press, N. J. & Frost, C. G. Catalytic meta-selective C–H functionalization to construct quaternary carbon centres. *Chem. Commun.* **51**, 12807–12810 (2015).
- Frost, C. G. & Paterson, A. J. Directing remote meta-C–H functionalization with cleavable auxiliaries. *ACS Cent. Sci.* **1**, 418–419 (2015).
- Hofmann, N. & Ackermann, L. meta-Selective C–H bond alkylation with secondary alkyl halides. *J. Am. Chem. Soc.* **135**, 5877–5884 (2013).
- Saidi, O. et al. Ruthenium-catalyzed meta sulfonation of 2-phenylpyridines. *J. Am. Chem. Soc.* **133**, 19298–19301 (2011).
- Ackermann, L., Hofmann, N. & Vicente, R. Carboxylate-assisted ruthenium-catalyzed direct alkylations of ketimines. *Org. Lett.* **13**, 1875–1877 (2011).
- Ruan, Z.-X. et al. Ruthenium(II)-catalyzed meta C–H mono- and difluoromethylations by phosphine/carboxylate cooperation. *Angew. Chem. Int. Ed.* **56**, 2045–2049 (2017).
- Li, Z.-Y. et al. Ruthenium-catalyzed meta-selective C–H mono- and difluoromethylation of arenes through ortho-metalation strategy. *Chem. Eur. J.* **23**, 3285–3290 (2017).
- Dey, A., Maity, S. & Maiti, D. Reaching the south: metal-catalyzed transformation of the aromatic para-position. *Chem. Commun.* **52**, 12398–12414 (2016).
- Zhao, Y., Yan, H., Lu, H., Huang, Z. & Lei, A.-W. para-Selective C–H bond functionalization of iodobenzenes. *Chem. Commun.* **52**, 11366–11369 (2016).
- Ciana, C.-L., Phipps, R. J., Brandt, J. R., Meyer, F.-M. & Gaunt, M. J. A highly para-selective copper(II)-catalyzed direct arylation of aniline and phenol derivatives. *Angew. Chem. Int. Ed.* **50**, 458–462 (2011).
- Ball, L. T., Lloyd-Jones, G. C. & Russell, C. A. Gold-catalyzed oxidative coupling of arylsilanes and arenes: origin of selectivity and improved precatalyst. *J. Am. Chem. Soc.* **136**, 254–264 (2014).
- Cambeiro, X. C., Boorman, T. C., Lu, P. & Larrosa, I. Redox-controlled selectivity of C–H activation in the oxidative cross-coupling of arenes. *Angew. Chem. Int. Ed.* **52**, 1781–1784 (2013).
- Ball, L. T., Lloyd-Jones, G. C. & Russell, C. A. Gold-catalyzed direct arylation. *Science* **337**, 1644–1648 (2012).
- Rosewall, C. F., Sibbald, Q. A., Liskin, D. V. & Michael, F. E. Palladium-catalyzed carboamination of alkenes promoted by N-fluorobenzenesulfonimide via C–H activation of arenes. *J. Am. Chem. Soc.* **131**, 9488–9489 (2009).
- Leitch, J. A. et al. Ruthenium-catalyzed para-selective C–H alkylation of aniline derivatives. *Angew. Chem. Int. Ed.* **56**, 15131–15135 (2017).
- Cheng, C. & Hartwig, J. F. Rhodium-catalyzed intermolecular C–H silylation of arenes with high steric regiocontrol. *Science* **343**, 853–857 (2014).
- Saito, Y., Segawa, Y. & Itami, K. para-C–H borylation of benzene derivatives by a bulky iridium catalyst. *J. Am. Chem. Soc.* **137**, 5193–5198 (2015).
- Wang, X., Leow, D. & Yu, J.-Q. Pd(II)-catalyzed para-selective C–H arylation of monosubstituted arenes. *J. Am. Chem. Soc.* **133**, 13864–13867 (2011).
- Yadagiri, D. & Anbarasan, P. Rhodium catalyzed direct arylation of  $\alpha$ -diazoamines. *Org. Lett.* **16**, 2510–2513 (2016).
- Yu, D.-G., de Azambuja, F. & Glorius, F. Direct functionalization with complete and switchable positional control: free phenol as a role model. *Angew. Chem. Int. Ed.* **53**, 7710–7712 (2014).
- Jia, S., Xing, D., Zhang, D. & Hu, W. Catalytic asymmetric functionalization of aromatic C–H bonds by electrophilic trapping of metal-carbene-induced zwitterionic intermediates. *Angew. Chem. Int. Ed.* **53**, 13098–13101 (2014).
- Yu, Z. et al. Highly site-selective direct C–H bond functionalization of phenols with  $\alpha$ -aryl- $\alpha$ -diazoacetates and diazooxindoles via gold catalysis. *J. Am. Chem. Soc.* **136**, 6904–6907 (2014).
- Cong, X. & Zeng, X. Iron-catalyzed, chelation-induced remote C–H allylation of quinolines via 8-amido assistance. *Org. Lett.* **16**, 3716–3719 (2014).
- Hu, X., Martin, D., Melaimi, M. & Bertrand, G. Gold-catalyzed hydroarylation of alkenes with dialkylanilines. *J. Am. Chem. Soc.* **136**, 13594–13597 (2014).
- Bag, S. et al. Remote para-C–H functionalization of arenes by a D-shaped biphenyl template-based assembly. *J. Am. Chem. Soc.* **137**, 11888–11891 (2015).
- Sun, K., Li, Y., Xiong, T., Zhang, J. & Zhang, Q. Palladium-catalyzed C–H aminations of anilides with N-fluorobenzenesulfonimide. *J. Am. Chem. Soc.* **133**, 1694–1697 (2011).
- Okumura, S. et al. para-Selective alkylation of benzamides and aromatic ketones by cooperative nickel/aluminum catalysis. *J. Am. Chem. Soc.* **138**, 14699–14704 (2016).
- Ma, B. et al. Highly para-selective C–H alkylation of benzene derivatives with 2,2,2-trifluoroethyl  $\alpha$ -aryl- $\alpha$ -diazoesters. *Angew. Chem. Int. Ed.* **56**, 2749–2753 (2017).
- Luan, Y.-X. et al. Amide-ligand-controlled highly para-selective arylation of monosubstituted simple arenes with arylboronic acids. *J. Am. Chem. Soc.* **139**, 1786–1789 (2017).
- Meanwell, N. A. Synopsis of some recent tactical application of bioisosteres in drug design. *J. Med. Chem.* **54**, 2529–2591 (2011).
- Purser, S., Moore, P. R., Swallow, S. & Gouverneur, V. Fluorine in medicinal chemistry. *Chem. Soc. Rev.* **37**, 320–330 (2008).
- Müller, F., Faeh, C. & Diederich, F. Fluorine in pharmaceuticals: looking beyond intuition. *Science* **317**, 1881–1886 (2007).
- O’Hagan, D. Understanding organofluorine chemistry. An introduction to the C–F bond. *Chem. Soc. Rev.* **37**, 308–319 (2008).
- Campbell, M. G. & Ritter, T. Modern carbon–fluorine bond forming reactions for aryl fluoride synthesis. *Chem. Rev.* **115**, 612–633 (2015).
- Nenajdenko, V. G., Muzalevskiy, V. M. & Shastin, A. V. Polyfluorinated ethanes as versatile fluorinated C2-building blocks for organic synthesis. *Chem. Rev.* **115**, 973–1050 (2015).
- Ni, C.-F., Hu, M. & Hu, J.-B. Good partnership between sulfur and fluorine: sulfur-based fluorination and fluoroalkylation reagents for organic synthesis. *Chem. Rev.* **115**, 765–825 (2015).
- Liang, T., Neumann, C. N. & Ritter, T. Introduction of fluorine and fluorine-containing functional groups. *Angew. Chem. Int. Ed.* **2013**, 8214–8264 (2013).
- Wan, X.-B. et al. Highly selective C–H functionalization/halogenation of acetanilide. *J. Am. Chem. Soc.* **128**, 7416–7417 (2016).
- Bedford, R. B., Haddow, M. F., Mitchell, C. J. & Webster, R. L. Mild C–H halogenation of anilides and the isolation of an unusual palladium(I)–palladium(II) species. *Angew. Chem. Int. Ed.* **50**, 5524–5527 (2011).

59. Gao, P. et al. Iridium(III)-catalyzed direct arylation of C–H bonds with diaryliodonium salts. *J. Am. Chem. Soc.* **137**, 12231–12240 (2015).
60. Xia, Y., Liu, Z., Feng, S., Zhang, Y. & Wang, J.-B. Ir(III)-catalyzed aromatic C–H bond functionalization via metal carbene migratory insertion. *J. Org. Chem.* **80**, 223–236 (2015).
61. Ackermann, L. Robust ruthenium(II)-catalyzed C–H arylations: carboxylate assistance for the efficient synthesis of angiotensin-II-receptor blockers. *Org. Process Res. Dev.* **19**, 260–269 (2015).
62. Li, B. & Dixneuf, P.H.  $sp^2$  C–H bond activation in water and catalytic cross-coupling reactions. *Chem. Soc. Rev.* **42**, 5744–5767 (2013).
63. Kitson, S. L., Jones, S., Watters, W., Chen, F. & Madge, D. Carbon-14 radiosynthesis of 4-(5-chloro-2-hydroxyphenyl)-3-(2-hydroxyethyl)-6-(trifluoromethyl)-[4- $^{14}C$ ]quinolin-2(1H)-one (XEN-D0401), a novel BK channel activator. *J. Label. Compd. Radiopharm.* **53**, 140–146 (2010).
64. Dai, H., Yu, C., Lu, C. & Yan, H. Rh<sup>III</sup>-catalyzed C–H allylation of amides and domino cyclization synthesis of 3,4-dihydroisoquinolin-1(2H)-ones with N-bromosuccinimide. *Eur. J. Org. Chem.* **2016**, 1255–1259 (2016).
65. Kondratov, L. S. et al. Radical reactions of alkyl 2-bromo-2,2-difluoroacetates with vinyl ethers: “Omitted” examples and application for the synthesis of 3,3-difluoro-GABA. *J. Org. Chem.* **80**, 12258–12264 (2015).
66. Crossley, S. W. M., Obradors, C., Martinez, R. & Shenvi, R. A. Mn-, Fe-, and Co-catalyzed radical hydrofunctionalizations of olefins. *Chem. Rev.* **116**, 8912–9000 (2016).
67. Streuff, J. & Gansäuer, A. Metal-catalyzed  $\beta$ -functionalization of Michael acceptors through reductive radical addition reactions. *Angew. Chem. Int. Ed.* **54**, 14232–14242 (2015).

## Acknowledgements

We gratefully acknowledge financial support from the Natural Science Foundation of China (Nos. 21772139, 21572149, 21772020, 21372266). The project of scientific and technologic infrastructure of Suzhou (SZS201708) and the PAPD Project are also gratefully acknowledged.

## Author contributions

Y.Z. directed the research. C.Y. and C.C. performed the experiments and analyzed the data. X.C. performed the transformations of **3a**. L.Z. and Y.L. performed the mechanism studies. Y.Z., Y.L., and Y.Y. prepared the manuscript.

## Additional information

**Supplementary Information** accompanies this paper at <https://doi.org/10.1038/s41467-018-03341-6>.

**Competing interests:** The authors declare no competing interests.

**Reprints and permission** information is available online at <http://npg.nature.com/reprintsandpermissions/>

**Publisher's note:** Springer Nature remains neutral with regard to jurisdictional claims in published maps and institutional affiliations.



**Open Access** This article is licensed under a Creative Commons Attribution 4.0 International License, which permits use, sharing, adaptation, distribution and reproduction in any medium or format, as long as you give appropriate credit to the original author(s) and the source, provide a link to the Creative Commons license, and indicate if changes were made. The images or other third party material in this article are included in the article's Creative Commons license, unless indicated otherwise in a credit line to the material. If material is not included in the article's Creative Commons license and your intended use is not permitted by statutory regulation or exceeds the permitted use, you will need to obtain permission directly from the copyright holder. To view a copy of this license, visit <http://creativecommons.org/licenses/by/4.0/>.

© The Author(s) 2018